New Journal of Physics
The open access journal at the forefront of physics

Deutsche Physikalische Gesellschaft DPG
IOP Institute of Physics

Published in partnership with: Deutsche Physikalische Gesellschaft and the Institute of Physics

OPEN ACCESS

RECEIVED
22 September 2016

REVISED
2 December 2016

ACCEPTED FOR PUBLICATION
9 December 2016

PUBLISHED
9 January 2017

PAPER

Anderson localization of composite excitations in disordered optomechanical arrays

Thales Figueiredo Roque[1], **Vittorio Peano**[2,3], **Oleg M Yevtushenko**[2,5] **and Florian Marquardt**[2,4]

[1] Instituto de Física Gleb Wataghin, Universidade Estadual de Campinas, 13083-859 Campinas, São Paulo, Brazil
[2] Institute for Theoretical Physics II, University Erlangen-Nürnberg, D-91058 Erlangen, Germany
[3] Department of Physics, University of Malta, Msida MSD 2080, Malta
[4] Max Planck Institute for the Science of Light, Günther-Scharowsky-Straße 1, D-91058 Erlangen, Germany
[5] Author to whom any correspondence should be addressed.

E-mail: Oleg.Yevtushenko@lmu.de

Keywords: optomechanics, localization, disordered structures

Supplementary material for this article is available online

Abstract

Optomechanical (OMA) arrays are a promising future platform for studies of transport, many-body dynamics, quantum control and topological effects in systems of coupled photon and phonon modes. We introduce disordered OMA arrays, focusing on features of Anderson localization of hybrid photon–phonon excitations. It turns out that these represent a unique disordered system, where basic parameters can be easily controlled by varying the frequency and the amplitude of an external laser field. We show that the two-species setting leads to a non-trivial frequency dependence of the localization length for intermediate laser intensities. This could serve as a convincing evidence of localization in a non-equilibrium dissipative situation.

Introduction

Optomechanics is a rapidly evolving research field at the intersection of condensed matter and quantum optics [1, 2]. By exploiting radiation forces, light can be coupled to the mechanical motion of vibration modes. The interplay of light and motion is now being used for a range of applications, from sensitive measurements to quantum communication, while it also turns out to be of significant interest for fundamental studies of quantum physics.

This rapidly developing area has so far mostly exploited the interaction between a single optical mode and a single mechanical mode. Going beyond this, recent theoretical research indicates the substantial promise of so-called optomechanical (OMA) arrays, where many modes are arranged in a periodic fashion. In such systems, a large variety of new phenomena and applications is predicted to become accessible in the future. These include the quantum many-body dynamics of photons and phonons [3], classical synchronization and nonlinear pattern formation [4–6], tunable long-range coupling of phonon modes [7–9], photon–phonon polariton bandstructures and transport [10, 11], artificial magnetic fields for photons [12], and topological transport of sound and light [13]. A first experimental realization of a larger-scale OMA array has recently been presented, involving seven coupled optical microdisks [14]. Even greater potential is expected for implementations based on OMA crystals [15–17], i.e photonic crystals that can be patterned specifically to generate localized photon and phonon modes.

Given these promising predictions and the rapid experimental progress towards larger arrays, the question of disorder effects now becomes of urgent importance. For example, in the case of OMA crystals, experiments indicate fluctuations in the geometry of about 1%, which translate into equally large relative fluctuations of both the mechanical and optical resonance frequencies. This will invariably have a very significant impact on the transport properties. However, gaining a better understanding of disorder effects in the various envisaged applications is only one motivation of the research to be presented here. Of equal, possibly even greater,

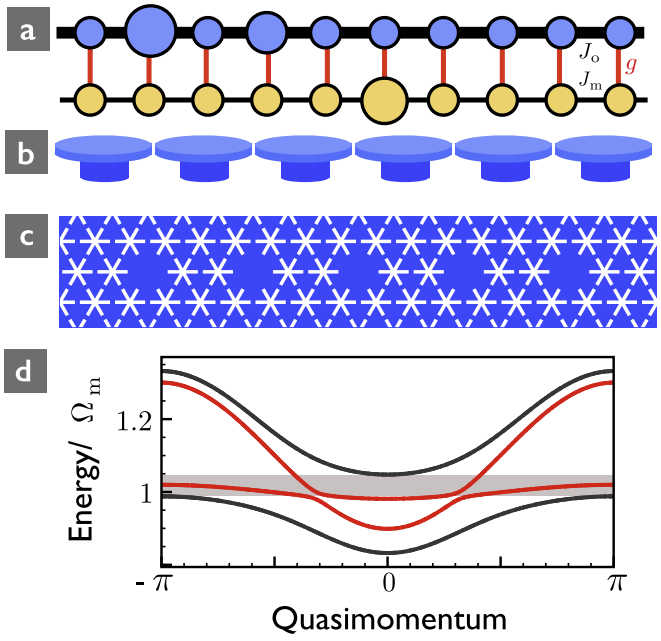

Figure 1. Scheme, implementations and band structure of an optomechanical array. (a) An array of photon (blue dots) and phonon (yellow) modes can be viewed as a ladder: photons and phonons either can hop to nearest neighbor sites or can be interconverted on the same site. This system can be implemented by (b) an array of microdisks, or (c) an array of co-localized optical and mechanical defect modes in an optomechanical crystal. (d) Optomechanical band structure for two different values of the coupling $g/\Omega_m = 0.01,\ 0.1$ (red/black lines). For the larger interaction strength the upper and lower polariton bands are separated by a complete band gap (gray region). The other parameters are $\Omega_o = 1.1\Omega_m$, $J_o = 0.1\Omega_m$, $J_m = 0.01\Omega_m$.

importance is the opportunity that is offered by optomechanics to create a highly tuneable novel platform for deliberately studying fundamental physical concepts such as Anderson localization [18].

Localization of waves in a random potential is one of the most remarkable and nontrivial interference effects. Initially, it has been studied in electronic disordered systems [19], though this effect applies equally to other types of quantum and even classical waves [20]. By now, localization and related phenomena have been discovered and investigated in photonic systems [21–28], coupled resonator optical waveguides [29], cold atomic gases [30, 31], in propagation of acoustic waves [32] and in Josephson junction chains [33]. Localization can even play a constructive role, namely in random lasing [28, 34]. In spite of extensive theoretical efforts, the unambiguous interpretation of experimental manifestations of localization often remains a challenge, even in situations where the archetypal version of Anderson localization applies.

OMA arrays enable controlled optical excitation and readout and at the same time promise significant flexibility in their design. However, it is the optical tuneability of the interaction between two different species (photons and phonons) that makes OMA systems a unique platform. As we will show in the present paper, this offers an opportunity to study effects in Anderson localization physics which currently represent a significant challenge even on the theoretical level and will thus open the door towards exploring novel physics that has not been observed so far.

The model

We consider a 1D array of OMA cells, see figure 1, driven by a single bright laser. The cell j contains an optical and a vibrational mode that are coupled via the standard linearized OMA Hamiltonian

$$\hat{H}_j = \sum_{\nu=o,m} \omega_{\nu,j}\, \hat{n}_{\nu,j} - g_j(\hat{c}_{o,j} + \hat{c}^\dagger_{o,j})(\hat{c}_{m,j} + \hat{c}^\dagger_{m,j}); \tag{1}$$

see [1][6] for details. Here $\hat{n}_{\nu,j} \equiv \hat{c}^\dagger_{\nu,j}\hat{c}_{\nu,j}$, and $\hat{c}_{\nu,j}$ is the bosonic annihilation operator of either optical, $\nu =$ 'o', or mechanical, $\nu =$ 'm', excitations (we set $\hbar = 1$). Due to disorder, the frequencies $\omega_{\nu,j}$ fluctuate around mean values $\langle\omega_{\nu,j}\rangle_d = \Omega_\nu$. We assume that $\omega_{\nu,j}$ are independent Gaussian random variables with variances $\langle(\omega_{\nu,j} - \Omega_\nu)(\omega_{\nu',j'} - \Omega_{\nu'})\rangle_d = \sigma^2_\nu \delta_{j,j'}\delta_{\nu,\nu'}$. Equation (1) is defined in a rotating frame, where the optical frequencies $\omega_{o,j}$ are counted off from the laser frequency, ω_L [1]. Thus, Ω_o indicates the average detuning and can be tuned *in situ* by varying the laser frequency. The OMA couplings g_j (with the mean value $g = \langle g_j\rangle_d$) are

[6] Derivation of the standard optomechanical Hamiltonian is briefly reviewed in Suppl.Mat.1.

proportional to the mean amplitude of the light circulating in the cavity j [1]. Hence, they are also tunable by varying the laser power.

The presence of two-mode squeezing interactions in equation (1) can in principle lead to instabilities. We choose Ω_o such that these terms are off-resonant and disorder configurations with optical [35] or vibrational instabilities are very rare. We leave their study for a forthcoming paper.

We can describe the full OMA by a Hamiltonian with nearest-neighbor optical, J_o, and mechanical, J_m, hopping amplitudes:

$$\hat{H} = \sum_j \hat{H}_j - \hat{H}_h, \quad \hat{H}_h = \sum_{j,\nu} J_\nu \hat{c}^\dagger_{\nu,j+1}\hat{c}_{\nu,j} + \text{H.c.} \tag{2}$$

Our model is time-reversal symmetric[7].

Clean polariton bands

In a clean OMA without dissipation (and without squeezing interaction), the photon–phonon hybridization leads to a pair of bands with energies

$$\Omega_\pm = \bar{\Omega} - 2\bar{J}\cos(k) \pm \sqrt{[\delta\Omega/2 - \delta J\cos(k)]^2 + g^2}, \tag{3}$$

where $\bar{\Omega} = (\Omega_o + \Omega_m)/2$, $\delta\Omega = (\Omega_o - \Omega_m)$ and likewise for $\bar{J}$, δJ. We refer to $\Omega_\pm$ as upper/lower polariton band, respectively. k denotes the wave-vector of polaritonic Bloch states. We focus on the regime where the uncoupled bands overlap, $\delta\Omega < 4\bar{J}$. In this case, the polariton bands are separated by a gap if the coupling becomes large enough, $g > g_{min}$,[8] see figure 1.

Anderson localization of uncoupled excitations

It is well known that even weak disorder leads to a crucial effect in a 1D system: the eigenstates become localized. If $g = 0$, each subsystem (photon/phonon), is individually described by the 1D Anderson model [18]. The localized states decay exponentially away from their center, $\sim\exp(-|j - j_0|/\xi^{(0)}_\nu)$. Here $\xi^{(0)}_{o,m}$ are the bare localization lengths for photons and phonons (for $g = 0$), measured in units of the lattice constant. Using the theory of 1D localization [36], we can approximate the frequency dependence of the localization length:

$$\xi^{(0)}_\nu(\Omega) \simeq 2(2\sin[k_\nu(\Omega)]/\chi_\nu)^2; \tag{4}$$

here the dimensionless quantities $\chi_\nu \equiv \sigma_\nu/J_\nu$ and $2\sin[k_\nu]$ are the disorder strength and the bare group velocity, respectively. Equation (4) is valid for weak (up to moderately strong) disorder[9]. The comparison of equation (4) with numerical results is shown below in figure 3.

In any experiment, localization can be detected if photons and phonons explore the localization length before leaking out, at a rate $\kappa_{o,m}$. This holds true if $\xi_\nu < 2J_\nu|\sin(k_\nu)|/\kappa_\nu$, which allows us to neglect dissipation in a first approximation[10]. In addition, the sample size L should be larger than the localization length, $L \gg \max(\xi^{(0)}_\nu)$. For typical $L \sim 100$ we need $\max(\xi^{(0)}_\nu) \sim 10$, corresponding to $\chi_\nu \sim 1$.

Localization in OMA arrays

At finite photon–phonon coupling, we encounter an Anderson model with two channels. Localization in the symmetric version of this model (with equal parameters of each channel) is well studied and understood [37, 38]. However, OMAs do not fall into this universality class since the mechanical band is generically much narrower than the optical one, $J_m \ll J_o$. Thus, the hybrid excitations consist of two components with very different velocities. Similar composite quasiparticles are not uncommon, another example is given by cavity polaritons [39, 40] including polaritons in a disordered potential [41]. Developing the theory of localization for such non-symmetric systems remains a real challenge, see [42]. The hybrid localized states typically have two localization lengths, $\xi_1 < \xi_2$, see the upper panel of figure 2. For small systems, $L < \xi_1$, the excitations do not feel localization and propagate ballistically. Their transmission decays as $\exp(-L/\xi_1)$ in the range $\xi_1 < L < \xi_2$ and becomes suppressed as $\exp(-L/\xi_2)$ at $L > \xi_2$. Our numerical analysis shows that the space region where ξ_1 dominates quickly shrinks with increasing g. Therefore, ξ_2 seems more interesting experimentally, and we will focus on this

[7] This means that $J_{o,m}$, g_0 and g are real.

[8] The value of g_{min} is found from the condition $\Omega_+(k = 0) = \Omega_-(k = \pi) \Rightarrow g_{min} = 2\,\mathrm{Re}\sqrt{J_o J_m(1 - [\delta\Omega/4\bar{J}]^2)}$.

[9] Strictly speaking, one must require $\chi_\nu < 1$ though a softer condition $\xi_\nu \gg 1$ sufficies for practical purposes.

[10] We have taken into account that, in 1D systems, the excitations propagate ballistically in the localization volume.

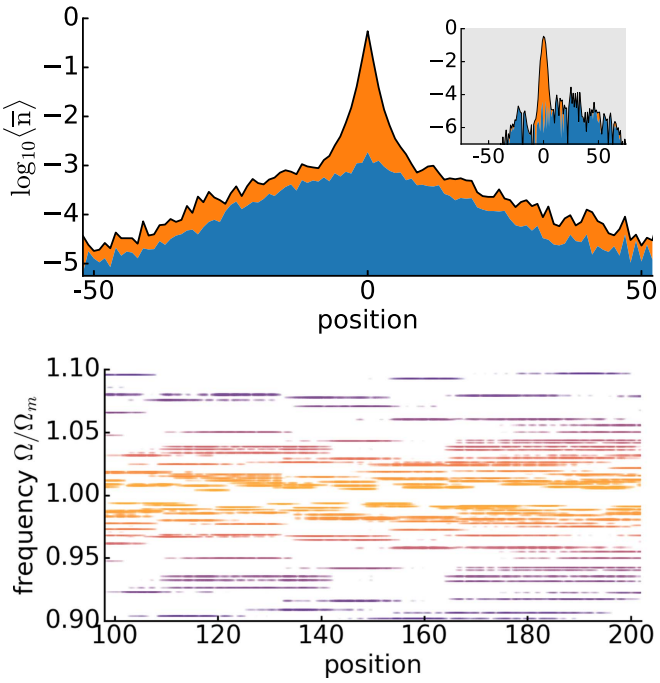

Figure 2. Upper panel: typical shape of an eigenstate, at $\Omega_o = \Omega_m$, $g = 0.001\Omega_m$, without disorder averaging (inset) and after disorder averaging over 500 realizations (main picture). Other parameters are explained in the text. Two different localization lengths are clearly visible. The profiles of $\bar{n}_j$, obtained from different disorder realizations, have been shifted in space, such that their maxima are always located at $j = 0$. Lower panel: local density of states (frequency-and position-resolved spectrum) at $g = 0.05\Omega_m$; other parameters as in the upper panel. The color ranges from orange to blue, depending on whether a given eigenstate has a stronger mechanical or optical component, respectively.

'large' localization length in the following. We start from a numerical analysis for relatively strong disorder. At the first stage, we neglect disorder-induced fluctuations of g_j [11] and use its homogeneous mean value $g = \text{const}$.

The method

The localization length can be obtained, e.g., from the photon–photon transmission, $T_{oo}(j, k; \Omega) \propto |G^R_{oo}(j, k; \Omega)|^2$ where $G^R_{oo}(j, k; \Omega) = -\mathrm{i}\int_0^\infty \mathrm{d}t \exp(\mathrm{i}\Omega t)\overline{[\hat{c}_{o,j}(t), \hat{c}^\dagger_{o,k}(0)]}$ is the frequency-resolved retarded Green's function. T_{oo} is defined via the optical power detected on site j at frequency $\omega_L + \Omega$ while a probe laser of the same frequency is impinging on a different site[12] k. For $x = |j - k| \to \infty$, we expect $T_{oo}(j, k; \Omega) \propto \exp(-2x/\xi_2)$. Thus, the expression for the averaged (inverse) localization length reads

$$\xi_2^{-1}(\Omega) = -\lim_{x\to\infty}(\langle \ln(T_{oo}(j, k; \Omega)\rangle_d / 2x). \tag{5}$$

We note that the value of $\xi_2(\Omega)$ is the same for other transmission processes (e.g. photon–phonon transmission) (see footnote 12).

Equation (5) can be used as a definition even in the presence of dissipation. In the absence of dissipation and instabilities, there is a simpler alternative, namely extracting the localization length directly from the spatial profile of eigenstates (see footnote 12). To ensure reliability of results, we have combined both approaches in numerical simulations.

Validity of the theory

Throughout our following analysis, we will concentrate on the particularly interesting regime of strong mode conversion which requires $|\Omega_o - \Omega_m| < \max\{J_o, \sigma_o\}$. Simultaneously, we assume that the mode squeezing is extremely weak which holds true if the terms $\hat{c}^\dagger_{o,j}\hat{c}^\dagger_{m,j}$ in the Hamiltonian (1) are not resonant and implies the following inequality $g, J_o, \sigma_o \ll \Omega_o$. In addition, the photon decay rate has to be small enough: $\kappa_o \ll \Omega_o, \Omega_m$.

[11] g_j is proportional to the mean occupation number of the photons on the site j while the cells with smaller optical frequencies host more photons. This locally enchances g_j on these sites.

[12] Algebraic details for the derivation of the localization radius can be found in Suppl.Mat.2.

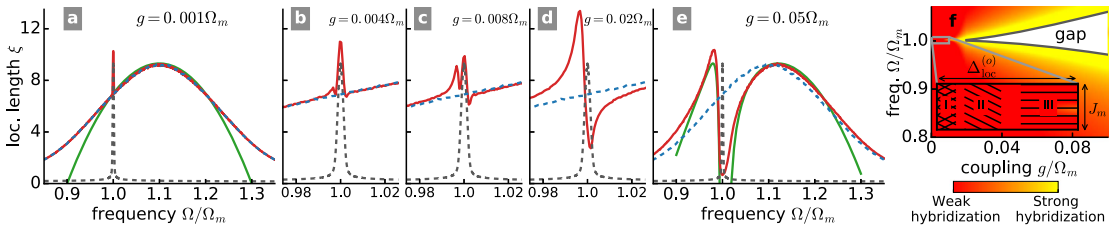

Figure 3. Frequency-dependence of the localization length: dashed lines show bare ($g = 0$) optical ($\xi_o^{(0)}$-blue) and mechanical ($\xi_m^{(0)}$-black) localization lengths. The red solid line shows the localization length of hybrid excitations, ξ, calculated at several values of the optomechanical coupling, $0.001\Omega_m \leqslant g \leqslant 0.05\Omega_m$, and $\Omega_o = 1.1\Omega_m$. Green solid lines describing $\xi_o^{(0)}$ in panel (a) and ξ in panel (e) are obtained from equations (4) to (6), respectively, after scaling by a constant factor. Panel (f) illustrates schematically the different regimes as a function of coupling and frequency. Colors denote different strength of the optomechanical hybridization, ranging from the perturbatively weak hybridization (red region) to the resonantly strong one (yellow region close to the gap of the clean bands, where the eigenmodes have simultaneously large optical and mechanical components).

We will study the possible influence of mode squeezing, for the regime where it may become relevant, in a forthcoming paper.

We note that our study does not include heating of the OMA cells produced by absorption of light [43], see explanations in Suppl.Mat.5.

Analysis of numerical results

The upper panel of figure 2 shows optical (blue shading) and mechanical (orange shading) components of a typical OMA eigenstate in the case of small coupling. The excitation frequency has been selected from the tail of the pure mechanical band. Two different slopes, which correspond to two different localization lengths $\xi_{1,2}$, are clearly visible. When g increases and the other parameters of the upper figure 2 remain unchanged, the region where ξ_1 dominates shrinks[13] and becomes invisible very quickly. In the following, we will concentrate on ξ_2 and will denote it as ξ for the sake of brevity. The lower panel of figure 2 illustrates the distribution of OMA excitations in space and frequency, including the character of excitations (photon versus phonon).

Here, and in the following, we have displayed numerical results for an illustrative set of parameters: $J_o = 0.1\Omega_m \gg J_m = 10^{-3}\Omega_m$. Localization of the OMA excitations becomes pronounced at $\chi_{o,m} \sim 1$. For concreteness, we have chosen equal relative disorder strength, $\chi_o = \chi_m = 1$. The OMAs which we study can be made from coupled optical disk resonators, see [14], or coupled defect modes in photonic–phononic crystals, see [15, 17], as well as in principle many other platforms. A geometrical disorder of about 1% has been observed in photonic–phononic crystals [44], leading to a relative disorder strength (ratio disorder to absolute frequency) of the same size both for the optical and mechanical modes. The disorder strength can also be reduced, if desired, by postfabrication techniques, which have been successful in reducing the disorder by at least two orders of magnitude [45]. In real samples implemented in OMA crystals, J_o ranges from 1 GHz to 10 THz (J_m: from 100 kHz to 1 GHz) with the optical disorder being of order 100 GHz to 1 THz (mechanical: from 10 MHz to 100 MHz), both in the absence of postprocessing. Thus, our choice of $\chi_{o,m}$ falls into the range of experimentally relevant parameters, if we assume postprocessing has been exploited to reduce the optical disorder by a factor 10^2–10^3. The OMA coupling in our numerics ranges from weak, $g = 10^{-3}\Omega_m$, to strong, $g = 0.05\Omega_m$. To suppress finite size effects, we employed large systems, $L = 10^3 \gg \xi$, during exact diagonalization. The Green's functions method has allowed us to explore even much larger sizes.

In figure 3, we display the frequency-dependence of the localization length of hybrid OMA excitations in a disordered array, one of the central numerical results of this article. For comparison, we also show the situation for the uncoupled systems, including the (scaled) analytical expression for $\xi_o^{(0)}$, equation (4)[14] (green solid line in figure 3(a)). Once the subsystems are coupled, significant changes of ξ (Ω) occur in the vicinity of the unperturbed (narrow) mechanical band where the OMA hybridization is most efficient. Firstly we note that, if $0 < g < \Delta_{loc}^{(m)}$, the coupling between the optical and the mechanical systems is perturbatively weak even in the middle of the mechanical band (region I in figure 3(f)). On the other hand, when the OMA coupling becomes large, $g > \sqrt{J_o J_m} = \sqrt{\sigma_o \sigma_m} \sim \Delta_{loc}^{(o)}$ for our choice of parameters, a gap opens around the resonant frequency

[13] If g increases and the other parameters of the upper figure 2 remain unchanged, ξ_2 slightly increases. This might lead to suppression of the region where ξ_1 dominates because the eigenstate is normalized.

[14] The accuracy of equation (4) is insufficient to reproduce the maximal value of $\xi_o^{(0)}(\Omega_o)$ at the relatively strong optical disorder, $\chi_o = 1$. Therefore, we have scaled the analytical answer by a constant factor to adjust the heights.

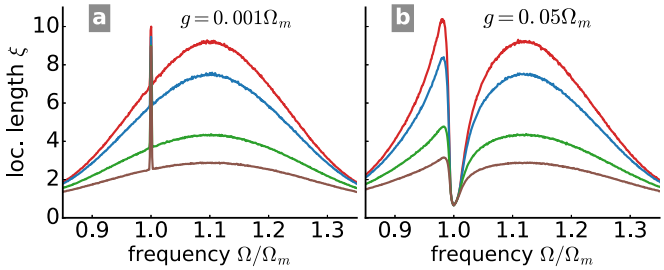

Figure 4. Frequency-dependence of the localization length at $\Omega_o = 1.1\Omega_m$ and $g/\Omega_m = \{0.001,\ 0.05\}$ calculated for different values of the optical decay rate $\kappa_o/\Omega_m = \{0,\ 0.01,\ 0.05,\ 0.1\}$ (red-, blue-, green-, and brown lines, respectively). Note that the peak at $g = 0.001\Omega_m$ and $\Omega = \Omega_m$ is almost insensitive to the optical dissipation since the corresponding wavefunctions have mainly mechanical components.

$\Omega = \Omega_m$ and excitations, which can be induced in the gap smeared by the disorder, become strongly localized (figure 3(e)).

Analytical methods which would allow one to explore localization in strongly disordered systems are not available in general. Nevertheless, it turns out that our OMA array corresponds to a certain two-channel system, which was studied analytically in [42] for the limit of weak disorder and large coupling. Remarkably, the shape of our numerically extracted $\xi(\Omega)$ at large g agrees with the predictions of [42], even though we are here dealing with strong disorder, $\chi_\nu \sim 1$ [38]. The theory of [42] is valid if g is large compared with the (bare) mean level spacing in the localization volume, $\Delta_{\rm loc}^{(\nu)}$, which holds true for the parameters of our numerical study at $g \geqslant 0.05\ \Omega_m$.[15] If $g > g_{\rm min}$, (i.e., if the clean polariton bands are separated by the gap of the width $\Omega_+(k=0) - \Omega_-(k=\pi)$) we can use the following (leading in χ_ν) expression for the localization length [42]:

$$\xi(\Omega) \simeq 4(2\sin[k_\pm(\Omega)])^2/(\chi^2[1+\cos^2(\gamma)]);$$
$$\tan(\gamma) = 2\sqrt{J_o J_m}\, g/\delta J\,(\Omega - \Omega_r), \quad \Omega_r \equiv J_o\delta\Omega/\delta J. \tag{6}$$

Here $\chi = \chi_o/\mathcal{C} = \chi_m/\mathcal{C}$ and $k_\pm(\Omega)$ denotes the inverted dispersion relation $\Omega_\pm(k)$. The quantity $V_\pm \equiv 2\sin[k_\pm(\Omega)]$ is called 'rapidity'. It coincides with the group velocity of the excitations for $g = 0$, and according to equation (6) it governs the frequency-dependence of $\xi(\Omega)$ in the coupled case. The factor $\mathcal{C}$ reflects renormalization of the disorder strength caused by the OMA coupling. Calculation of $\mathcal{C}$ is beyond the scope of [42] and we have found its approximate value $\mathcal{C} \simeq 1.16$ by fitting the analytically calculated maximal value of $\xi(\Omega > \Omega_m)$ to the numerical one. Figure 3(e) shows the comparison of the analytical and numerical results. They differ noticeably only close to edges of the clean band where the analytical theory looses its validity because $\xi \to 1$. In addition, the gap is smeared by the relatively strong disorder.

We have discovered that, at $\Omega \simeq \Omega_m$, the crossover between small and large values of g is highly non-trivial (and it is outside the scope of the analytical theory): when the OMA coupling increases from $g \sim \Delta_{\rm loc}^{(m)}$ to $g \sim J_m$ (region II in figure 3(f)), the single maximum of ξ (see figures 3(a)→(b)) grows sublinearly in g[16]. This growth stops and turns into a decrease when $g \gg J_m$. Simultaneously, a new local maximum develops at the frequency corresponding to the maximum of the rapidity (figures 3(b)→(c) and region III in figure 3(f)). Finally, the new local maximum becomes the global one and a dip appears close to Ω_m at $g \geqslant \Delta_{\rm loc}^{(o)}$ (figures 3(c)→(d)). This non-trivial dependence of the localization length on the coupling constant, i.e., on the tuneable intensity of the external laser, could help to distinguish localization and trivial dissipation effects in real experiments.

We have checked that the shape of $\xi(\Omega)$ is robust with respect to dissipation effects (related to the energy leakage) as long as the mean level spacing in the localization volume of the hybrid excitations is larger than the optical and mechanical decay rates, κ_ν,[17]. Propagation of the excitations is suppressed due to their finite life time which is reflected by the frequency-independent decrease of ξ. Typical profiles $\xi(\Omega)$ are shown in figure 4 where the optical dissipation rate increases until $\kappa_o = 0.1\Omega_m$. These profiles are also robust with respect to the spatial inhomogeneity of g_j (see footnotes 11 and 18) and κ_o; both effects can result, for example, from a randomness of geometry of the individual OMA cells. In particular, we have confirmed by numerical simulations (not shown

[15] The mean level spacing in the localization volume is obtained from the relation $\Delta_{\rm loc}/\Delta = N/\xi$. Using the estimate for the mean level spacing in a band of extremely localized states $\Delta \sim \delta/N$ [46, 47], we find $\Delta_{\rm loc}^{(\nu)} \sim \delta_\nu/\xi_\nu^{(0)} \sim J_\nu/\xi_\nu^{(0)}$. Here $\xi_\nu^{(0)}$ denotes bare (at $g = 0$) localization lengths. For the chosen parameters, this yields the condition $g > 10^{-1}\max\{J_\nu\} \sim 10^{-2}\Omega_m$. Thus, the analytical theory from [42] can be used to understand the case $g = 0.05\Omega_m$ while smaller values of g are beyond the validity range of the analytic expressions.

[16] The increase of $\xi_2(\Omega \simeq \Omega_m)$ when the optomechanical coupling is small, $g < J_m$, is explained in Suppl.Mat.3.

[17] Equivalently, we can require that the localization length is much smaller than the escape length.

[18] This robustness is exemplified in Suppl.Mat.4.

here) that fluctuations of the optical dissipation of order $\delta\kappa_o/\kappa_o \sim \sigma_o/\Omega_o \sim 0.1$ do not have any noticeable effect on the results presented in figure 4.

Conclusions and discussion

Disordered OMAs belong to a new class of disordered systems where composite (photon–phonon) excitations are localized and the most important parameters can be easily fine-tuned. Thus, OMAs provide a unique opportunity to study Anderson localization of composite particles in real experiments. Moreover, they should allow to reliably distinguish localization from trivial dissipation effects. Future studies may address the additional novel physics that will arise when two-mode squeezing processes become relevant. At strong driving, this could involve the interplay between instabilities and localization, with interesting connections to random lasing, extending the new research domain of disordered OMA arrays into the nonlinear regime.

Acknowledgments

We acknowledge support from the EU Research Council through the grant EU-ERC OPTOMECH 278320. TFR acknowledges support from FAPESP. We are grateful to Vladimir Kravtsov, Denis Basko and Igor Yurkevich for useful discussions.

References

[1] Aspelmeyer M, Kippenberg T and Marquardt F 2014 *Rev. Mod. Phys.* **86** 1391
[2] Aspelmeyer M, Groeblacher S, Hammerer K and Kiesel N 2010 *J. Opt. Soc. Am.* B **27** A189
[3] Ludwig M and Marquardt F 2013 *Phys. Rev. Lett.* **111** 073603
[4] Heinrich G, Ludwig M, Qian J, Kubala B and Marquardt F 2011 *Phys. Rev. Lett.* **107** 043603
[5] Holmes C A, Meaney C P and Milburn G J 2012 *Phys. Rev.* E **85** 066203
[6] Lauter R, Brendel C, Habraken S J M and Marquardt F 2015 *Phys. Rev.* E **92** 012902
[7] Xuereb A, Genes C and Dantan A 2012 *Phys. Rev. Lett.* **109** 223601
[8] Xuereb A, Genes C, Pupillo G, Paternostro M and Dantan A 2014 *Phys. Rev. Lett.* **112** 133604
[9] Schmidt M, Ludwig M and Marquardt F 2012 *New J. Phys.* **14** 125005
[10] Chen W and Clerk A A 2014 *Phys. Rev.* A **89** 033854
[11] Schmidt M, Peano V and Marquardt F 2015 *New J. Phys.* **17** 023025
[12] Schmidt M, Kessler S, Peano V, Painter O and Marquardt F 2015 *Optica* **2** 635
[13] Peano V, Brendel C, Schmidt M and Marquardt F 2015 *Phys. Rev.* X **5** 031011
[14] Zhang M, Shah S, Cardenas J and Lipson M 2015 *Phys. Rev. Lett.* **115** 163902
[15] Safavi-Naeini A H, Alegre T P M, Winger M and Painter O 2010 *Appl. Phys. Lett.* **97** 181106
[16] Chan J, Safavi-Naeini A H, Hill J T, Meenehan S and Painter O 2012 *Appl. Phys. Lett.* **101** 081115
[17] Safavi-Naeini A H, Hill J T, Meenehan S, Chan J, Gröblacher S and Painter O 2014 *Phys. Rev. Lett.* **112** 153603
[18] Anderson P W 1958 *Phys. Rev.* **109** 1492
[19] Kramer B and MacKinnon A 1993 *Rep. Prog. Phys.* **56** 1469
[20] van Rossum M C W and Nieuwenhuizen T M 1999 *Rev. Mod. Phys.* **71** 313
[21] Chabanov A A, Stoytchev M and Genack A Z 2000 *Nature* **404** 850
[22] Schwartz T, Bartal G, Fishman S and Segev M 2007 *Nature* **446** 52
[23] Mookherjea S, Park J S, Yang S-H and Bandaru P R 2008 *Nat. Photon.* **2** 90
[24] Lahini Y, Avidan A, Pozzi F, Sorel M, Morandotti R, Christodoulides D N and Silberberg Y 2008 *Phys. Rev. Lett.* **100** 013906
[25] Savona V 2011 *Phys. Rev.* B **83** 085301
[26] Martin L *et al* 2011 *Opt. Express* **19** 13636
[27] Segev M, Silberberg Y and Christodoulides D N 2013 *Nat. Photon.* **7** 197
[28] Liu J, Garcia P D, Ek S, Gregersen N, Suhr T, Schubert M, Mørk J, Stobbe S and Lodahl P 2014 *Nat. Nanotechnol.* **9** 285
[29] Hafezi M, Demler E A, Lukin M D and Taylor J M 2011 *Nat. Phys.* **7** 907–12
[30] Billy J, Josse V, Zuo Z, Bernard A, Hambrecht B, Lugan P, Clement D, Sanchez-Palencia L, Bouyer P and Aspect A 2008 *Nature* **453** 891
[31] Roati G, D'Errico C, Fallani L, Fattori M, Fort C, Zaccanti M, Modugno G, Modugno M and Inguscio M 2008 *Nature* **453** 895
[32] Hu H F, Strybulevych A, Page J H, Skipetrov S E and van Tiggelen B A 2008 *Nat. Phys.* **4** 945
[33] Basko D M and Hekking F W J 2013 *Phys. Rev.* B **88** 094507
[34] Wiersma D S 2008 *Nature* **4** 359
[35] Mandel L and Wolf E 2008 *Optical Coherence and Quantum Optics* (Cambridge: Cambridge University Press)
[36] Melnikov V I 1981 *Sov. Phys. Solid State* **23** 444
[37] Dorokhov O N 1982 *Solid State Commun.* **44** 915
[38] Mello P A and Kumar N 2004 *Quantum Transport in Mesoscopic Systems* (Oxford: Oxford University Press.)
[39] Kasprzak J *et al* 2006 *Nature* **443** 409
[40] Wertz E *et al* 2010 *Nat. Phys.* **6** 860
[41] Manni F, Lagoudakis K G, Pietka B, Fontanesi L, Wouters M, Savona V, Andre R and Deveaud-Pledran B 2011 *Phys. Rev. Lett.* **106** 176401
[42] Xie H-Y, Kravtsov V E and Müller M 2012 *Phys. Rev.* B **86** 014205
[43] Meenehan S M, Cohen J D, Gröblacher S, Hill J T, Safavi-Naeini A H, Aspelmeyer M and Painter O 2014 *Phys. Rev.* A **90** 011803

[44] Painter O private communication
[45] Fang K, Luo J, Metelmann A, Matheny M H, Marquardt F, Clerk A A and Painter O 2016 *Nat. Phys.* (arXiv:1608.03620)
[46] Yevtushenko O and Kravtsov V E 2003 *J. Phys. A: Math. Gen.* **36** 8265
[47] Yevtushenko O and Kravtsov V E 2004 *Phys. Rev.* E **69** 026104